Determination of Temperatures and Heat Fluxes on Surfaces and Interfaces of Multidomain Three-Dimensional Electronic Components

Brian H. Dennis
e-mail: dennis@garlic.q.t.u-tokyo.ac.jp
Institute of Environmental Studies, Graduate School of Frontier Sciences, University of Tokyo, 7-3-1 Hongo, Bunkyo-ku, Tokyo 113-8656, Japan

Zhen-xue Han
e-mail: han@uta.edu
Department of Mechanical and Aerospace Engineering, UTA Box 19018, University of Texas at Arlington, Arlington, TX 76019

George S. Dulikravich
e-mail: dulikrav@fiu.edu
Mechanical and Materials Engineering Department, Florida International University, 10555 W. Flagler Street, Miami, FL 33174

A finite element method (FEM) formulation for the prediction of unknown steady boundary conditions in heat conduction for multidomain three-dimensional (3D) solid objects is presented. The FEM formulation is capable of determining temperatures and heat fluxes on the boundaries where such quantities are unknown, provided such quantities are sufficiently overspecified on other boundaries. An inverse finite element program has been previously developed and successfully tested on 3D simple geometries. The finite element code uses an efficient sparse matrix storage scheme that allows treatment of realistic 3D problems on personal computer. The finite element formulation also allows for very straightforward treatment of geometries composed of many different materials. The inverse FEM formulation was applied to the prediction of die-junction temperature distribution in a simple ball grid array electronic package. Examples are presented with simulated measurements, which include random measurement errors. Regularization was applied to control numerical error when large measurement errors were added to the overspecified boundary conditions. [DOI: 10.1115/1.1827261]

Introduction

It is often difficult and even impossible to place temperature probes or heat flux probes on certain parts of a solid body surface. This can be either due to its small size, geometric inaccessibility, or because of exposure to a hostile environment. With an appropriate inverse method these unknown boundary values can be deduced from additional information, which should be made available at a finite number of points within the body or on some other surfaces of the solid body. In the case of steady heat conduction, the objective of an inverse boundary condition determination problem is to compute the temperatures and heat fluxes on any surfaces or surface elements where such information is unknown [1]. The problem of inverse determination of unknown boundary conditions in two-dimensional steady heat conduction has been solved by a variety of methods [1–5]. Similarly, a separate inverse boundary condition determination problem in linear elastostatics has been solved by different methods [6].

For inverse problems, the unknown boundary conditions on parts of the boundary can be determined by overspecifying the boundary conditions (enforcing both Dirichlet- and Neumann-type boundary conditions) on at least some of the remaining portions of the boundary and providing either Dirichlet- or Neumann-type boundary conditions on the rest of the boundary. It is possible, after a series of algebraic manipulations, to transform the original system of equations into a system that enforces the overspecified boundary conditions and includes the unknown boundary conditions as a part of the unknown solution vector. This formulation is an adaptation of a method by Martin and Dulikravich [4] for the inverse detection of boundary conditions in steady heat conduction.

Our objective is to demonstrate the inverse FEM approach for the simultaneous determination of thermal boundary conditions and interface temperatures for electronic packages. In particular, we focus on the inverse determination of the junction temperature distribution on the microchip, typically called a die. The die junction temperature is a critical quantity in the design of electronic packaging. The package should be designed so that the junction temperature always stays within a specified range. It is difficult to directly measure junction temperature because the die is typically completely encased within the electronic package. However, it can be inversely determined using only temperature and heat flux measurements on the outer surface of the package. In the case of ball grid array (BGA) packages, the temperatures and heat fluxes cannot be easily obtained on the bottom due to the small dimensions of the air gap. Therefore, we must rely solely on measurements taken from the top and sides of the package.

Manuscript received April 26, 2004; revision received April 28, 2004. Review conducted by: B. Sammakia.

FEM Formulation for Heat Conduction

The temperature distribution throughout the domain can be found by solving the Poisson equation for steady linear heat conduction with a distributed steady heat source function S and thermal conductivity coefficients k_x, k_y, k_z

$$\frac{\partial}{\partial x}\left(k_x\frac{\partial\Theta}{\partial x}\right)+\frac{\partial}{\partial y}\left(k_y\frac{\partial\Theta}{\partial y}\right)+\frac{\partial}{\partial z}\left(k_z\frac{\partial\Theta}{\partial z}\right)=-S \tag{1}$$

Applying the method of weighted residuals to (1) over an element results in

$$\int_{\Omega^e} v\left(k_x\frac{\partial^2\Theta}{\partial x^2}+k_y\frac{\partial^2\Theta}{\partial y^2}+k_z\frac{\partial^2\Theta}{\partial z^2}-S\right)d\Omega^e=0 \tag{2}$$

where v is a nonzero weight function. Integrating Eq. (2) by parts once, creates the weak statement for an element

$$-\int_{\Omega^e}\left(k_x\frac{\partial v}{\partial x}\frac{\partial\Theta}{\partial x}+k_y\frac{\partial v}{\partial y}\frac{\partial\Theta}{\partial y}+k_z\frac{\partial v}{\partial z}\frac{\partial\Theta}{\partial z}\right)d\Omega^e$$

$$=\int_{\Omega^e} vSd\Omega^e-\int_{\Gamma^e} v(\vec{q}\cdot\vec{n})d\Omega^e \tag{3}$$

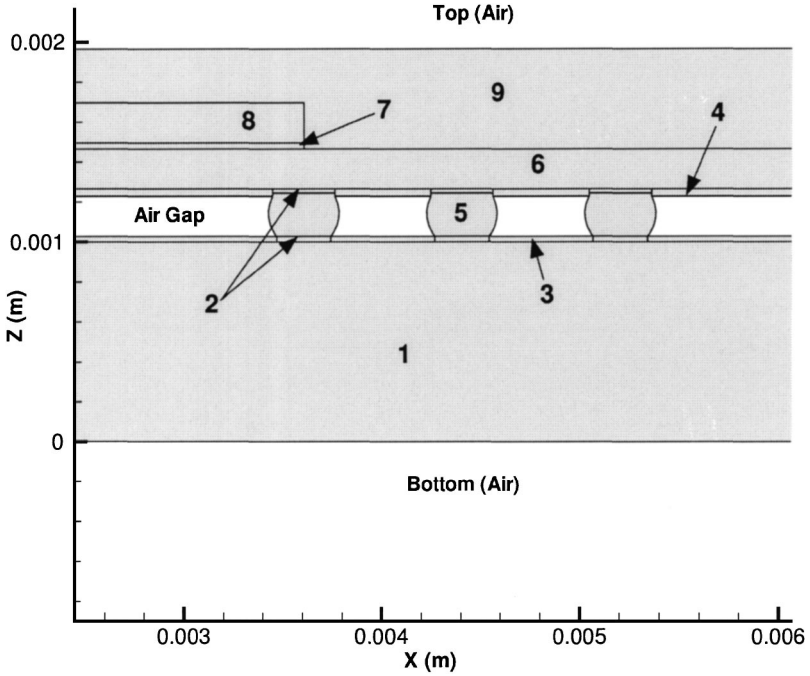

Fig. 1 Cross section showing material regions for BGA model

Variation of the temperature and the weight function across an element with m nodes can be expressed by

$$\Theta^e(x,y,z)=\sum_{i=1}^{m} N_i(x,y,z)\Theta_i^e=\{N\}^T\{\Theta^e\} \tag{4}$$

$$v^e(x,y,z)=\sum_{i=1}^{m} N_i(x,y,z)v_i^e=\{N\}^T\{v^e\} \tag{5}$$

where the functions N_i for v^e and Θ^e are chosen to be the same. This is known as a Galerkin finite element approach. The functions v^e and Θ^e are substituted into Eq. (3), leading to a discrete weak statement. The discrete weak statement is then made stationary with respect to the weight function coefficients v_i, resulting in a system of linear equations for the element. By first defining the matrix [B],

$$[B]=\begin{bmatrix} \frac{\partial N_1}{\partial x} & \frac{\partial N_2}{\partial x} & \cdots & \frac{\partial N_m}{\partial x} \\ \frac{\partial N_1}{\partial y} & \frac{\partial N_2}{\partial y} & \cdots & \frac{\partial N_m}{\partial y} \\ \frac{\partial N_1}{\partial z} & \frac{\partial N_2}{\partial z} & \cdots & \frac{\partial N_m}{\partial z} \end{bmatrix} \tag{6}$$

the linear system of equations can be written in matrix form as

$$[K_c^e]\{\Theta^e\}=\{Q^e\} \tag{7}$$

where

$$[K_c^e]=\int_{\Omega^e}[B]^T[k][B]d\Omega^e \tag{8}$$

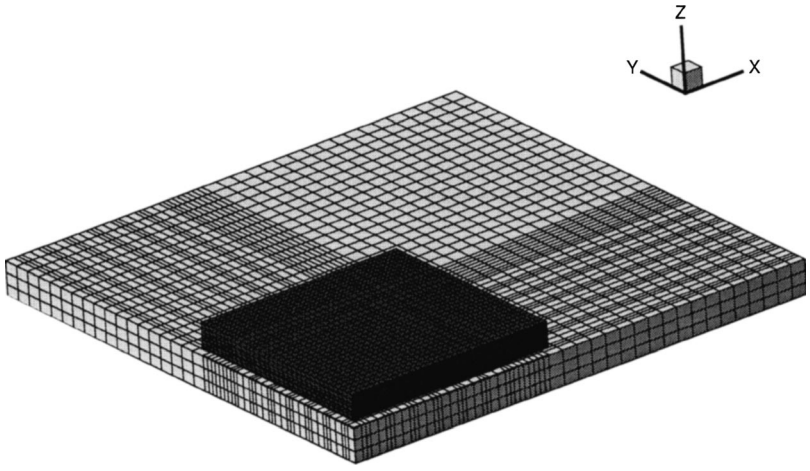

Fig. 2 Hexahedral mesh for PWB and EMC

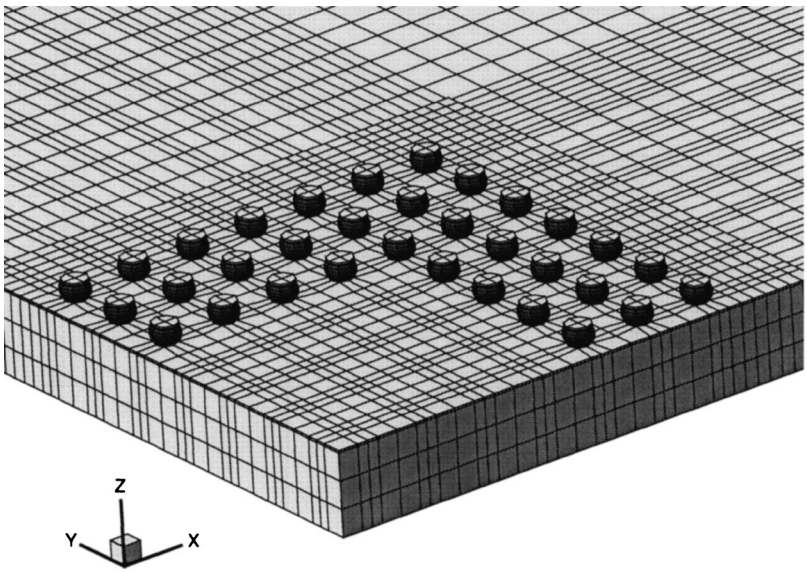

Fig. 3 Closeup view of mesh for solder balls, solder mask, and PWB

$$\{Q^e\} = -\int_{\Omega^e} S\{N\}d\Omega + \int_{\Gamma^e} q_s\{N\}d\Gamma^e \tag{9}$$

$$[k] = \begin{bmatrix} k_x & 0 & 0 \\ 0 & k_y & 0 \\ 0 & 0 & k_z \end{bmatrix} \tag{10}$$

The local stiffness matrix $[K_c^e]$ and heat flux vector $\{Q^e\}$ are determined for each element in the domain and then assembled into the global system of linear algebraic equations

$$[K_c]\{\Theta\} = \{Q\} \tag{11}$$

Direct and Inverse Formulations

The above equations for steady heat conduction were discretized by using a Galerkin finite element method. The system is typically large, sparse, symmetric, and positive definite. Once the global system has been formed, the boundary conditions are applied. For a well-posed analysis (direct) problem, the boundary conditions must be known on all domain boundaries. For heat conduction, either the temperature Θ_s or the heat flux Q_s must be specified at each point of the boundary.

For an inverse problem, the unknown boundary conditions on parts of the boundary can be determined by overspecifying the boundary conditions (enforcing both Dirichlet- and Neumann-type boundary conditions) on at least some of the remaining portions of the boundary and providing either Dirichlet- or Neumann-type boundary conditions on the rest of it. It is possible, after a series of algebraic manipulations, to transform the original system of equations into a system that enforces the overspecified boundary conditions and includes the unknown boundary conditions as part of the unknown solution vector. As an example, consider the linear system for heat conduction on a tetrahedral finite element with boundary conditions given at nodes 1 and 4,

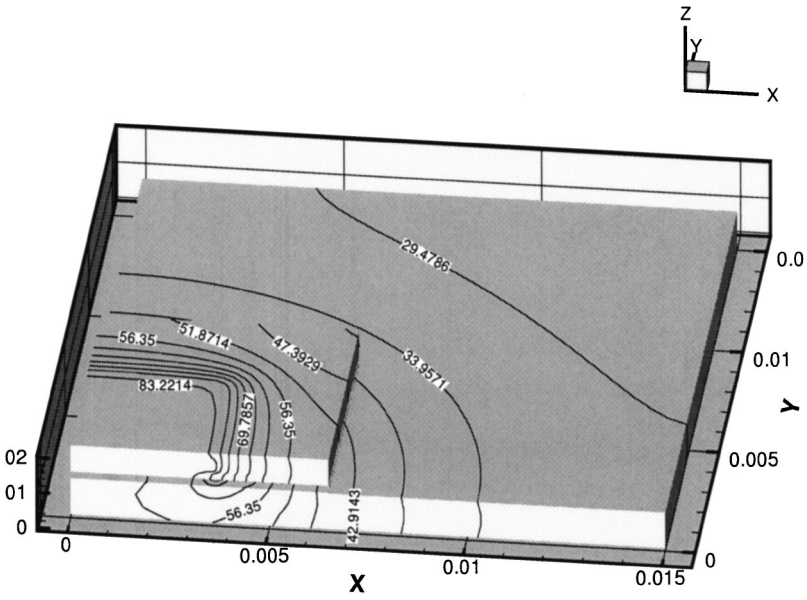

Fig. 4 Computed temperature on PWB and EMC

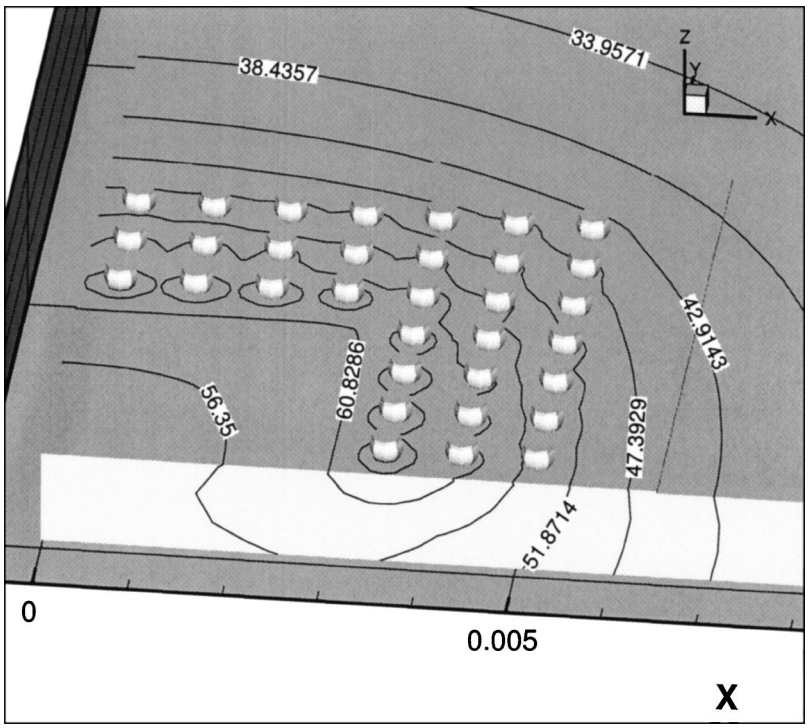

Fig. 5 Computed temperature on solder balls, solder mask, and PWB

$$\begin{bmatrix} K_{11} & K_{12} & K_{13} & K_{14} \\ K_{21} & K_{22} & K_{23} & K_{24} \\ K_{31} & K_{32} & K_{33} & K_{34} \\ K_{41} & K_{42} & K_{43} & K_{44} \end{bmatrix} \begin{Bmatrix} \Theta_1 \\ \Theta_2 \\ \Theta_3 \\ \Theta_4 \end{Bmatrix} = \begin{Bmatrix} Q_1 \\ Q_2 \\ Q_3 \\ Q_4 \end{Bmatrix} \tag{12}$$

As an example of an inverse problem, one could specify both the temperature Θ_s and the heat flux Q_s at node 1, flux only at nodes 2 and 3, and assume the boundary conditions at node 4 as being unknown. The original system of equations (12) can be modified by adding a row and a column corresponding to the additional equation for the overspecified flux at node 1 and the additional unknown due to the unknown boundary flux at node 4,

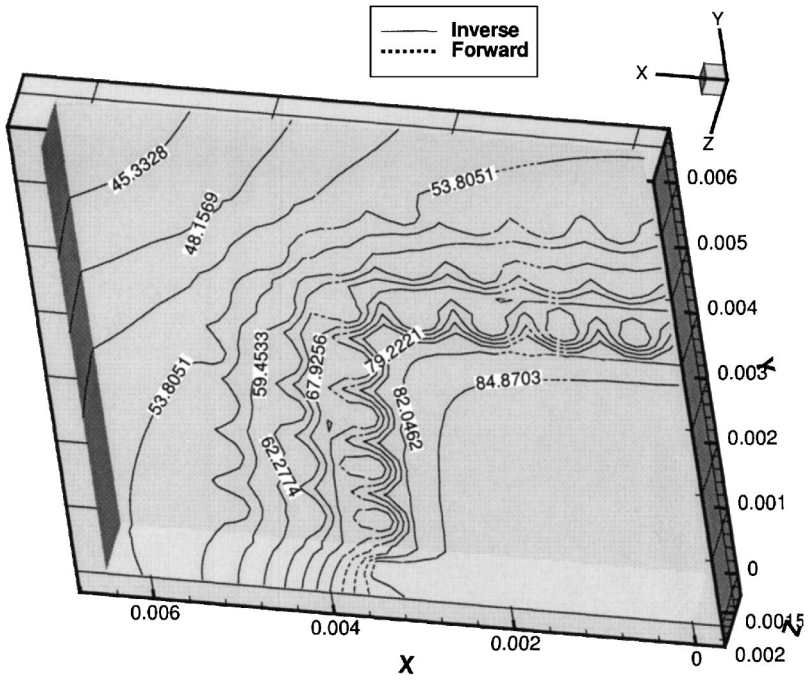

Fig. 6 Computed inverse and forward temperature on BT substrate bottom

$$\begin{bmatrix} 1 & 0 & 0 & 0 & 0 \\ K_{21} & K_{22} & K_{23} & K_{24} & 0 \\ K_{31} & K_{32} & K_{33} & K_{34} & 0 \\ K_{41} & K_{42} & K_{43} & K_{44} & -1 \\ K_{11} & K_{12} & K_{13} & K_{14} & 0 \end{bmatrix} \begin{Bmatrix} \Theta_1 \\ \Theta_2 \\ \Theta_3 \\ \Theta_4 \\ Q_4 \end{Bmatrix} = \begin{Bmatrix} \Theta_s \\ Q_2 \\ Q_3 \\ 0 \\ Q_s \end{Bmatrix} \quad (13)$$

The resulting systems of equations will remain sparse, but will be unsymmetric and possibly rectangular depending on the ratio of the number of known to unknown boundary conditions.

Regularization

A regularization method is needed when the overspecified boundary conditions contain some amount of error. The Tikhonov regularization [7] method is the most widely used approach. However, our previous research has shown that higher-order regularization methods result in more accurate solutions to inverse boundary condition problems [1,8].

The general form of a regularized system is given as [9]

$$\begin{bmatrix} K_c \\ \Lambda D \end{bmatrix} \{\Theta\} = \begin{Bmatrix} Q \\ 0 \end{Bmatrix} \quad (14)$$

where the traditional Tikhonov regularization is obtained when the damping matrix $[D]$ is set equal to the identity matrix. Solving (14) in a least-squares sense minimizes the following error function:

$$error(\Theta) = \|[K_c]\{\Theta\} - \{Q\}\|_2^2 + \|\Lambda[D]\{\Theta\}\|_2^2 \quad (15)$$

This is the minimization of the residual plus a penalty term. The form of the damping matrix determines what penalty is used, and the damping parameter Λ weights the penalty for each equation. These weights should be determined according to the measurement error associated with the respective equation. The Tikhonov approach clearly drives the solution to zero as the damping parameter increases. For this reason, we avoid using the Tikhonov regularization method in inverse boundary detection problems.

The method used here is essentially a Laplacian smoothing of the unknown temperatures on the boundaries where the boundary conditions are unknown. This method could be considered a ''second-order'' Tikhonov method. A penalty term can be constructed such that curvature of the solution on the unspecified boundary is minimized along with the residual,

$$\|\nabla^2 \Theta_{ub}\|_2^2 \rightarrow \min \quad (16)$$

Equation (16) is discretized using the method of weighted residuals to determine the damping matrix $[D]$,

$$\|[D]\Theta_{ub}\|_2^2 = \|[K_c]\Theta_{ub}\|_2^2 \quad (17)$$

In three-dimensional problems, $[K_c]$ is computed by integrating over surface elements on the unknown boundaries. So the damping matrix can be thought of as an assembly of boundary elements that make up the surface of the object where the conditions are unknown. The stiffness matrix for each boundary element is formed by using a Galerkin weighted-residual method, which ensures the Laplacian of the solution is minimized over the unknown boundary surface. The main advantage of this method is its ability to smooth the solution vector without necessarily driving the components to zero and away from the true solution.

Numerical Results

The finite element inverse formulation was shown previously to be both accurate and efficient for several three-dimensional test problems [8,10]. The method has been implemented in an object-oriented finite element code written in C++. The software uses sparse matrix storage that allows 3D problems to be solved on a personal computer in less than a few minutes. All the inverse cases presented here were computed in less than three minutes on 2.0 GHz P4 Xeon processor and required less than 120 MB memory. Elements used in the calculations were hexahedra with trilinear interpolation functions. The linear system was solved with a sparse QR factorization [11].

Table 1 Material properties for BGA model

Region	Material	k_x, k_y, k_z (W/m °C)
1	FR4 printed wire board (PWB)	1.0, 1.0, 0.3
2	copper pads	393.0, 393.0, 393.0
3	solder mask	0.2, 0.2, 0.2
4	polyimide tape	0.3, 0.3, 0.3
5	solder balls	250.0, 250.0, 250.0
6	bismaleimide triazene (BT) substrate	1.0, 1.0, 0.3
7	die attach	0.25, 0.25, 0.25
8	silicon die	87.0, 87.0, 87.0
9	epoxy mold compound (EMC)	0.71, 0.71, 0.71

Table 2 Boundary conditions for forward problem

Boundary	Θ_{amb} (°C)	h (W/m^2 °C)
Symmetry	0.0	0.0
All sides of PWB	25.0	19.71
Top and sides of package	25.0	43.18
Bottom of package	25.0	4.31
Sides of solder balls	0.0	0.0

A simplified BGA geometry with nine material domains was generated for a test case. The x-y dimensions were 30.0 mm $\times$30.0 mm for the printed wire board (PWB), 13.0 mm$\times$13.0 mm for the package, and 7.2 mm$\times$7.2 mm for the die. The dimensions in the z direction should be discernible from Fig. 1. Though the generated geometry is not an actual BGA package, we tried to make a model that maintains the characteristic shape and material domains of a typical BGA electronic package. Specifically, this model does not include the traces that carry the electrical signals through the PWB and the package to the die. The material regions are shown in Fig. 1, and their properties are listed in Table 1. The BGA geometry is symmetric with respect to the x and y axes. In this simplified example we assume the boundary conditions have the same symmetry as well. Therefore, only a quarter of the BGA model was used for computations. A hexahedral mesh was generated for the quarter geometry and was composed of 27,417 nodes and 20,728 elements. The surface mesh for the BGA geometry is shown in Figs. 2–3.

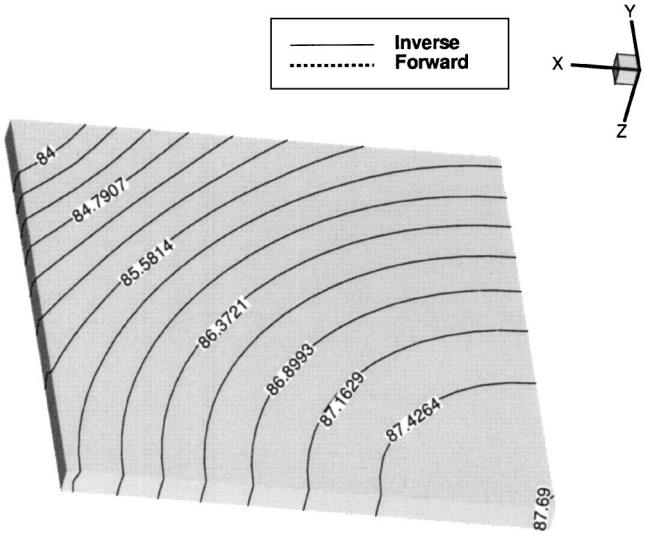

Fig. 7 Computed inverse and forward temperature on die bottom

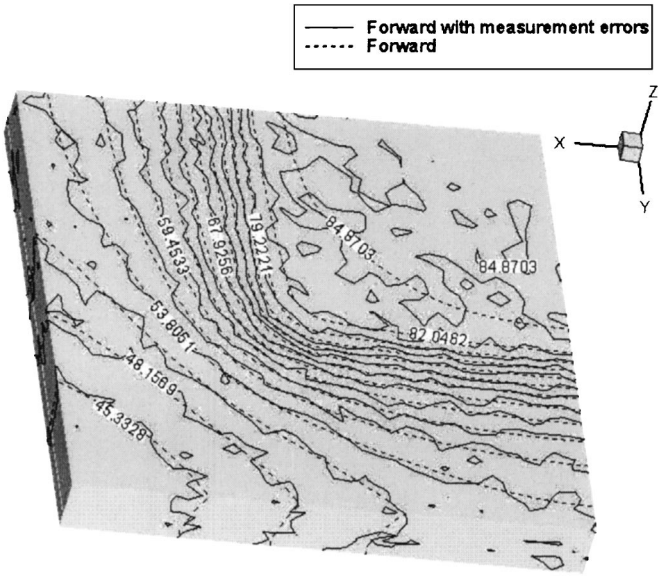

Fig. 8 Computed forward temperature on package top with measurement errors

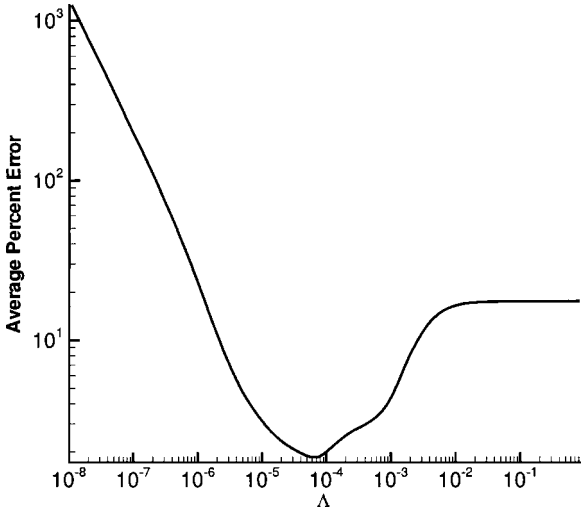

Fig. 9 Variation of average relative error in temperature on BT substrate bottom

In the examples presented here, the overspecified boundary condition measurements were simulated by taking them from a well-posed finite element analysis of the entire BGA model. For the well-posed or forward-analysis problem, the boundary conditions were specified on all boundaries of the mesh. The power source in the quarter model of the die was set to 0.1875 W and was uniformly distributed. The forward problem was then solved using convection-type boundary conditions with values given in Table 2. The computed temperature field is shown in Figs. 4–5.

We were primary interested in determining the junction temperature on the surface of the silicon die. This was accomplished economically by modeling only regions 6–9 and then overspecifying the boundary conditions on the top and sides of the package. No boundary conditions were specified on the bottom of the BT substrate. In this case, only the mesh for regions 6–9 was required for solving the inverse problem. The reduced grid contained 9800 nodes and 8092 elements, about three times smaller than the complete BGA grid.

The inverse problem was then created by overspecifying the top and sides of the package with the double-precision values of temperatures and fluxes obtained from the forward-analysis case. At

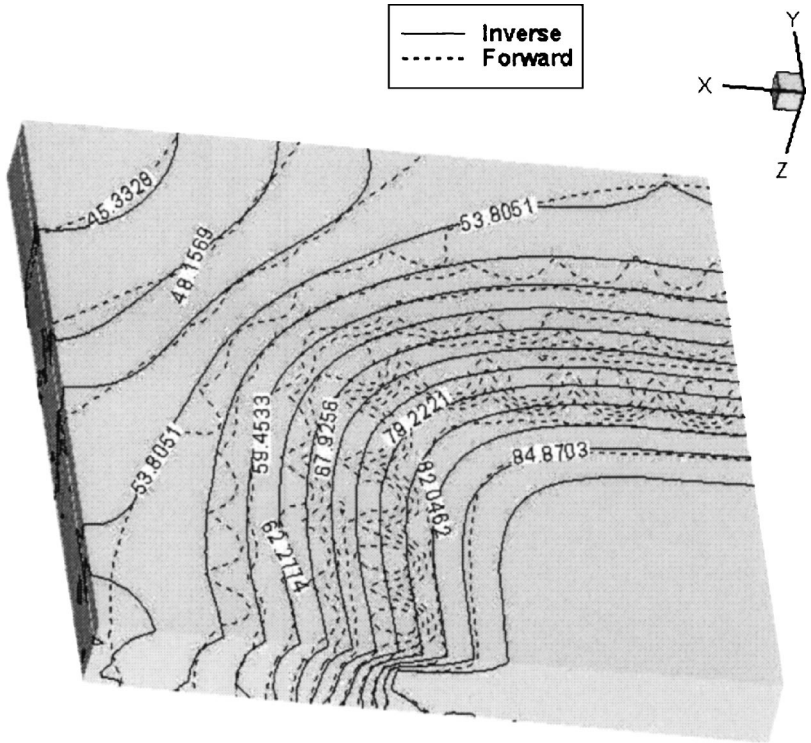

Fig. 10 Computed inverse and forward temperature on BT substrate bottom with measurement errors and $\Lambda = 1.0 \times 10^{-4}$

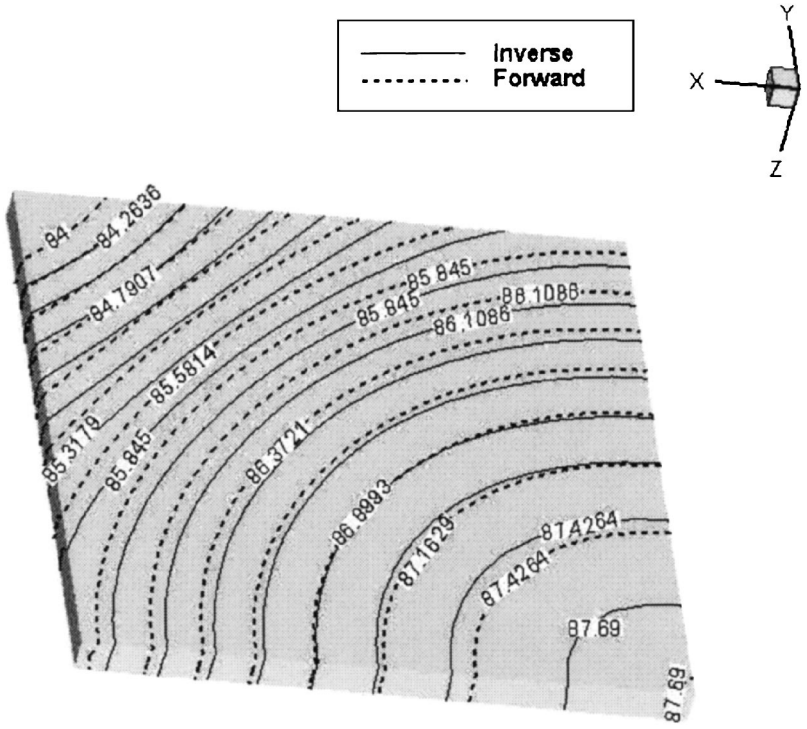

Fig. 11 Computed inverse and forward temperature on die bottom with measurement errors and $\Lambda = 1.0 \times 10^{-4}$

the same time, no boundary conditions were specified on the bottom of region 6. Random measurement errors were not used in this case. The heat source magnitude, its distribution, and all material properties were assumed to be known. A damping parameter of $\Lambda = 1.0 \times 10^{-30}$ was used. The computed forward and inverse temperature distribution on the bottom of the BT substrate is shown in Fig. 6. The average relative error in temperature between the forward analysis and inverse result was less than 0.005%. The inverse procedure also accurately predicted the temperature distribution on the bottom of the silicon die as shown in Fig. 7.

The above problem was repeated using overspecified boundary conditions with random measurement errors added. Random errors in the known boundary temperatures and fluxes were generated using the following equations [4]:

$$\Theta = \Theta_{bc} \pm \sqrt{-2\overline{\sigma^2} \ln R} \tag{18}$$

$$Q = Q_{bc} \pm \sqrt{-2\overline{\sigma^2} \ln R} \tag{19}$$

where R is a uniform random number between 0.0 and 1.0 and $\overline{\sigma}$ is the standard deviation. Equations (18) and (19) were used to generate errors in both the known boundary fluxes and temperatures obtained from the forward solution.

In a final test case, a value of $\overline{\sigma} = 0.01$ was used with Eqs. (18) and (19) to generate random errors. This resulted in an average measurement error of 1.27% in the overspecified temperatures and 1.24% for the overspecified fluxes. The overspecified temperatures with errors are shown in Fig. 8. The inverse problem was solved for various values of the damping parameter Λ. Figure 9 shows that the relative temperature error on the unknown boundary is less than 3.0% for $1.0 \times 10^{-5} < \Lambda < 1.0 \times 10^{-3}$. The results show that the regularization successfully prevents the amplification of the measurement errors, provided the appropriate damping parameter is used. The computed forward and inverse temperature distribution on the bottom of the BT substrate for $\Lambda = 1.0 \times 10^{-4}$ is shown in Fig. 10. The smoothing effect of the regularization can be clearly seen. Although the fine details of the temperature field are not recovered, the general distribution is captured correctly. The average relative error in temperatures on the bottom of the BT substrate surface was 2.00%. The inverse procedure also predicted a temperature distribution on the die with less than 2.0% average error as shown in Fig. 11. Again, the inverse and forward solutions do not match exactly due to the presence of the measurement errors. However, the errors in the die temperature are of the same order of magnitude as the measurement errors, thereby indicating that the regularization method is working successfully.

Conclusions

A formulation for the inverse determination of unknown steady boundary conditions in heat conduction for three-dimensional multidomain problems has been demonstrated. The formulation has been successfully applied to the inverse detection of the die junction temperature distribution for a BGA electronic package with nine material domains. The method computed the temperature distribution in the die and package with high accuracy when no measurement errors were present in the overspecified boundary conditions. The method required regularization when measurement errors were added to the boundary conditions. However, it was demonstrated that a high-order regularization method successfully prevented the amplification of the measurement errors. Relatively accurate die junction temperatures were computed even for average measurement errors exceeding 1%.

Acknowledgment

The authors are grateful for the partial support provided for this research from the Grant No. NSF DMS-0073698 administered through the Computational Mathematics program.

Nomenclature

Γ = boundary surface
Λ = damping parameter
Ω^e = element volume

$\bar{\sigma}$ = standard deviation
Θ = temperature
Θ_{amb} = ambient fluid temperature
$[D]$ = damping matrix
h = heat convection coefficient
k_x, k_y, k_z = Fourier coefficients of heat conduction in x, y, z
$\vec{n}$ = surface unit normal vector
$\vec{q}$ = heat flux
q_s = normal heat flux
R = uniform random number between 0 and 1
S = heat source
x, y, z = Cartesian body axes

References

[1] Dennis, B. H., and Dulikravich, G. S., 1999, ''Simultaneous Determination of Temperatures, Heat Fluxes, Deformations, and Tractions on Inaccessible Boundaries,'' ASME J. Heat Transfer, **121**(1), pp. 537–545.

[2] Larsen, M. E., 1985, ''An Inverse Problem: Heat Flux and Temperature Prediction for a High Heat Flux Experiment,'' Tech. Rep. SAND-85-2671, Sandia National Laboratories, Albuquerque, NM.

[3] Hensel, E. H., and Hills, R., 1989, ''Steady-State Two-Dimensional Inverse Heat Conduction,'' Numer. Heat Transfer, Part A, **15**, pp. 227–240.

[4] Martin, T. J., and Dulikravich, G. S., 1996, ''Inverse Determination of Boundary Conditions in Steady Heat Conduction,'' ASME J. Heat Transfer, **3**, pp. 546–554.

[5] Olson, L. G., and Throne, R. D., 2000, ''The Steady Inverse Heat Conduction Problem: A Comparison for Methods of Inverse Parameter Selection,'' 34th National Heat Transfer Conference-NHTC'00, Paper No. NHTC2000-12022, Pittsburg.

[6] Martin, T. J., Halderman, J., and Dulikravich, G. S., 1995, ''An Inverse Method for Finding Unknown Surface Tractions and Deformations in Elastostatics,'' Comput. Struct., **56**, pp. 825–836.

[7] Tikhonov, A. N., and Arsenin, V. Y., 1977, *Solutions of Ill Posed Problems*, Wistom and Sons, Washington, DC.

[8] Dennis, B. H., and Dulikravich, G. S., 2001, ''A 3-D Finite Element Formulation for the Determination of Unknown Boundary Conditions in Heat Conduction,'' *Proc. of International Symposium on Inverse Problems in Engineering Mechanics*, M. Tanaka, ed., Nagano City, Japan.

[9] Neumaier, A., 1998, ''Solving Ill-Conditioned and Singular Linear Systems: A Tutorial on Regularization,'' SIAM Rev., **40**, pp. 636–666.

[10] Dennis, B. H., Dulikravich, G. S., and Yoshimura, S., 2003, ''A Finite Element Formulation for the Determination of Unknown Boundary Conditions for 3-D Steady Thermoelastic Problems,'' ASME J. Heat Transfer, (submitted).

[11] Matstoms, P., 1991, ''The Multifrontal Solution of Sparse Least Squares Problems,'' Ph.D. thesis, Linköping University, Sweden.